Applied Physics Letters

# Effects of ferroelectric-poling-induced strain on magnetic and transport properties of $La_{0.67}Ba_{0.33}MnO_3$ thin films grown on (111)-oriented ferroelectric substrates

Cite as: Appl. Phys. Lett. **103**, 132910 (2013); https://doi.org/10.1063/1.4822269
Submitted: 20 April 2013 . Accepted: 08 September 2013 . Published Online: 26 September 2013

Q. X. Zhu, M. Zheng, M. M. Yang, X. M. Li, Y. Wang, X. Shi, H. L. W. Chan, H. S. Luo, X. G. Li, and R. K. Zheng

# Effects of ferroelectric-poling-induced strain on magnetic and transport properties of $La_{0.67}Ba_{0.33}MnO_3$ thin films grown on (111)-oriented ferroelectric substrates

Q. X. Zhu,[1] M. Zheng,[1] M. M. Yang,[1] X. M. Li,[1,a)] Y. Wang,[2] X. Shi,[1] H. L. W. Chan,[2] H. S. Luo,[1] X. G. Li,[3] and R. K. Zheng[1,b)]
[1]*State Key Laboratory of High Performance Ceramics and Superfine Microstructure, Shanghai Institute of Ceramics, Chinese Academy of Sciences, Shanghai 200050, China*
[2]*Department of Applied Physics and Materials Research Center, The Hong Kong Polytechnic University, Hong Kong, China*
[3]*Hefei National Laboratory for Physical Sciences at Microscale and Department of Physics, University of Science and Technology of China, Hefei 230026, China*

(Received 20 April 2013; accepted 8 September 2013; published online 26 September 2013)

$La_{0.67}Ba_{0.33}MnO_3$ thin films were epitaxially grown on (111)-oriented $0.31Pb(In_{1/2}Nb_{1/2})O_3$-$0.35Pb(Mg_{1/3}Nb_{2/3})O_3$-$0.34PbTiO_3$ ferroelectric single-crystal substrates. During ferroelectric poling and polarization rotation, the resistance of $La_{0.67}Ba_{0.33}MnO_3$ films tracks the electric-field-induced in-plane strain of substrates effectively, implying strain-mediated coupling. Upon poling along the [111] direction, ferromagnetism is suppressed for $T < 175$ K, but enhanced for $T > 175$ K, which is explained by magnetoelastic coupling that modifies the film's magnetic anisotropy. Our findings also show that the magnetic field has an opposite effect on the strain-tunability of resistance [i.e.,$(\Delta R/R)_{strain}$] above and below the Curie temperature $T_C$, which is interpreted within the framework of phase separation. © *2013 AIP Publishing LLC*. [http://dx.doi.org/10.1063/1.4822269]

Theoretical and experimental studies have shown that multiferroic heterostructures composed of epitaxial manganite thin films on ferroelectric single crystals (e.g., $(1-x)Pb(Mg_{1/3}Nb_{2/3})O_3$-$xPbTiO_3$ (PMN-$x$PT),[1–10] and $BaTiO_3$[11–13]) exhibit magnetoelectric effect, mediated by interfacial strain coupling that can be achieved by applying an electric field to PMN-$x$PT or $BaTiO_3$. Apart from the strain-mediated mechanism, recent experimental investigations on heterostructures consisting of ferromagnetic and ferroelectric double-layered thin films revealed that the magnetoelectric effect can be driven by accumulation/depletion of charge carriers at interface (i.e., ferroelectric field effect), arising from electric-field-induced remnant polarization in ferroelectric layer.[14–17] For manganite films epitaxially grown on ferroelectric single crystals, the electric-field-induced strain and ferroelectric field effect are anticipated to influence the lattice strain and charge carrier density, respectively, and thus have significant impact on the electronic transport and magnetic properties of manganite films.[18]

Over the past few years, (001)-[2,3,7–10] and (011)-oriented[4–6] ferroelectric single crystals (PMN-$x$PT) ($0.28 \leq x \leq 0.33$) with attractive ferroelectric and piezoelectric properties have been adopted to compose ferromagnetic film/PMN-$x$PT heterostructures. However, (111)-oriented PMN-$x$PT single crystals have not been employed as ferroelectric substrates. Modifying the physical properties of manganite films on (111)-oriented ferroelectric single crystals is yet to be studied.

Herein, we report the epitaxial growth of $La_{0.67}Ba_{0.33}MnO_3$ (LBMO) thin films on (111)-oriented $0.31Pb(In_{1/2}Nb_{1/2})O_3$-$0.35Pb(Mg_{1/3}Nb_{2/3})O_3$-$0.34PbTiO_3$ (PIN-PMN-PT) ternary ferroelectric single crystals, possessing tetragonal structure,[19] weak ferroelectricity [inset (e) of Fig. 1] and piezoelectricity ($d_{33} \sim 100$ pC/N). The LBMO film adjusts its lattice strain to the lattice change experienced by PIN-PMN-PT upon poling or polarization rotation. The film resistance tracks the electric-field-induced strain of the substrate effectively at room temperature, exhibiting strain-mediated coupling. Opposing effects by the magnetic field on the strain effect and strain-induced modulations of the magnetic state are demonstrated and explained in terms of phase separation and magnetic anisotropy, respectively.

LBMO films were deposited on polished PIN-PMN-PT substrates by pulsed laser deposition during which the substrate temperature and $O_2$ pressure were kept at 700 °C and 25 Pa, respectively. Film thickness was measured to be ~30 nm using a JSM-6700F scanning electron microscope. Atomic force microscopy [inset (b) of Fig. 1] reveals a rather flat surface of the film, with a root-mean-square roughness of ~1 nm. X-ray diffraction (XRD) $\theta$–$2\theta$ and $\phi$ scans were recorded on a four-circle Bruker D8 Discover X-ray diffractometer, equipped with Cu $K_{\alpha 1}$ radiation. Electric-field-induced variation in the out-of-plane strain for LBMO film was measured by XRD. Electric-field-induced in-plane strain for PIN-PMN-PT was monitored using a TC-32 K Handheld Data Logger (Tokyo Sokki Kenkyujo Co., Ltd.). Ferroelectric poling and polarization rotation were conducted by applying electric fields to PIN-PMN-PT substrate through the bottom and top Au electrodes at $T = 300$ K, as shown in inset (a) of Fig. 1. The film resistance was measured using a physical property measurement system (PPMS-9, Quantum Design). Magnetic properties were characterized using a superconducting quantum interference device (MPMS XL-5, Quantum Design) magnetometer.

The XRD $\theta$–$2\theta$ scan pattern in Fig. 1 shows that the LBMO film is of single phase and (111) preferentially

a)lixm@mail.sic.ac.cn
b)zrk@ustc.edu

 

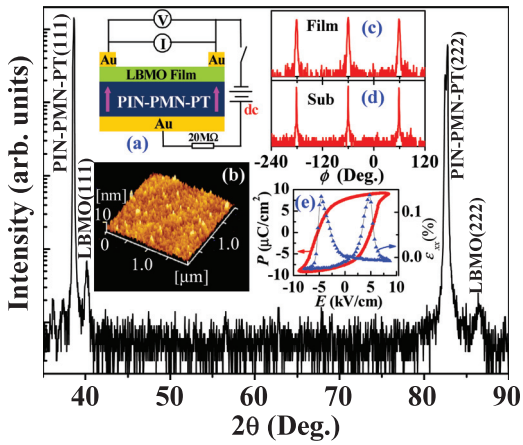


FIG. 1. XRD pattern of LBMO/PIN-PMN-PT. (a) Measurement circuit for LBMO/PIN-PMN-PT structure. (b) Surface morphology of LBMO film. (c) and (d) XRD $\phi$ scans of the LBMO (101) and PIN-PMN-PT (101) diffraction peaks, respectively. (e) Polarization and in-plane strain versus $E$ for PIN-PMN-PT.

oriented. The XRD $\phi$-scan patterns of the LBMO (101) and PIN-PMN-PT (101) planes exhibit trifold symmetry [insets (c) and (d) in Fig. 1, respectively], disclosing a clear cube-on-cube epitaxial growth of LBMO film on PIN-PMN-PT substrate. Both PIN-PMN-PT and LBMO bulk materials possess a pseudocubic unit cell with lattice parameters $a \sim b \sim c \sim 4.02$ Å for the former and $a \sim b \sim c \sim 3.92$ Å for the latter. For coherent epitaxial growth of LBMO film on PIN-PMN-PT substrate, LBMO film should be subjected to in-plane tensile strain and out-of-plane compressive strain. The calculated lattice spacing $d$ (~2.24 Å) for the LBMO (111) plane is indeed smaller than the bulk value (~2.26 Å).

In order to observe the effects of substrate poling along the [111] direction on the electronic transport properties, the film resistance was measured as a function of electric field ($E$) applied to the unpoled PIN-PMN-PT substrate at $T = 300$ K. The relative change in resistance $\Delta R/R$ during the poling process is shown in Fig. 2. $\Delta R/R$ is defined as $\Delta R/R = [R(E) - R(0)]/R(0)$, where $R(E)$ and $R(0)$ represent the resistance of LBMO film under applied and zero $E$, respectively. $\Delta R/R$ is mostly constant for $E < 2.7$ kV/cm, but decreases sharply with increasing $E$ from 2.7 to 3.3 kV/cm. For

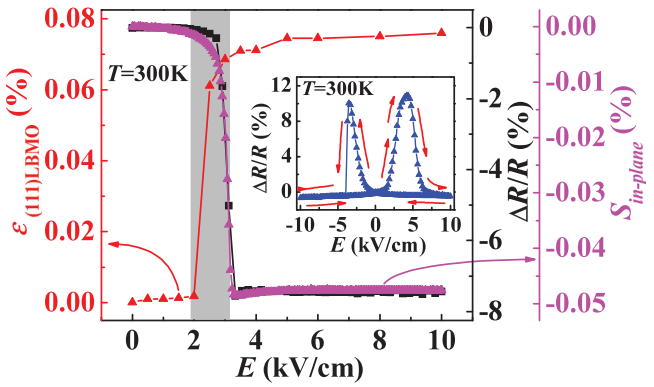


FIG. 2. Electric-field-induced $\Delta R/R$ and out-of-plane strain of the LBMO film, and in-plane strain of PIN-PMN-PT as a function of $E$ applied to PIN-PMN-PT. Inset: $\Delta R/R$ of the LBMO film at $T = 300$ K as a function of bipolar $E$ applied to PIN-PMN-PT.

$E > 3.3$ kV/cm, $\Delta R/R$ is largely independent of $E$, probably because of the weak converse piezoelectricity of the tetragonal (111)-oriented PIN-PMN-PT.[19] The variation in $\Delta R/R$ tracks the electric-field-induced in-plane compressive strain ($S_{\text{in-plane}}$) in the PIN-PMN-PT substrate effectively, intuitively implying that it is the strain transferred from the PIN-PMN-PT substrate to the LBMO film that modifies the electronic transport properties of the LBMO film. As is known, the spontaneous polarization direction for a tetragonal phase is along [001] with six equivalent orientations. Upon polarization along the [111] direction, non-180° ferroelectric domain reorientation gives rise to a nonlinear change in strain near the coercive field. The induced strain is transferred to the LBMO film, causing a release of in-plane tensile strain. Thus, there is an increase in $d$ along the [111] direction (see Fig. 2), as manifested by the shift of the LBMO (111) diffraction peak towards lower angle under $E = 10$ kV/cm (not shown). At $E = 10$ kV/cm, the out-of-plane strain of the LBMO film increases by ~0.076% (see $\varepsilon_{111(LBMO)}$ in Fig. 2). This strain-induced modification of transport properties can be ascribed to the strain-induced weakening of electron-lattice coupling and strengthening of the double-exchange interaction.[3]

A more direct visualization of the strain effect is shown in the inset of Fig. 2, which shows $\Delta R/R$ as a function of bipolar $E$ applied to PIN-PMN-PT at $T = 300$ K. $\Delta R/R$ versus $E$ curve exhibits a typical butterfly-like shape as the polarization direction is switched, resembling the butterfly-like strain versus $E$ loop of PIN-PMN-PT shown in inset (e) of Fig. 1. This further confirms strain-induced nature of the resistance change. The bipolar strain loop in inset (e) of Fig. 1 suggests that a non-180° polarization reorientation occurs near the coercive field, and produces a large jump in strain near $E_C$. With further increase in the reversed $E$, polarization undergoes another non-180° reorientation. This two-stage polarization reversal results in a 180° switch for all domains. Consequently, little difference was found in the strain between the positively poled $P_r^+$ (i.e., electric dipole moments point upward, see inset (a) of Fig. 1) and negatively poled $P_r^-$ states. As a result, the discrepancy between the film resistance for the $P_r^+$ and $P_r^-$ states is extremely small (see inset of Figs. 2 and 3). It is known that polarization direction switching induces an accumulation of positive or negative electric charge at interface between the film and the substrate, which can be screened by an equal number of charge carriers of opposite sign within the film, thereby changing the film's doping level. If the ferroelectric field effect plays an important role, the resistance of the LBMO film would be modified by polarization direction reversal. Actually, the resistance for the $P_r^+$ state is similar to that for the $P_r^-$ state, suggesting that the polarization-switching-induced electrostatic doping effect is minor and can be disregarded.

Figure 3 shows the temperature dependence of the resistance for the LBMO film under $H = 0$, 3 and 7 T when PIN-PMN-PT is in an unpoled $P_r^0$, $P_r^+$, and $P_r^-$ states, respectively. Similar to reported manganite thin films with optimal doping level,[12] the LBMO film exhibits an insulator-to-metal transition near the Curie temperature $T_C$, where the ferromagnetic metallic (FMM) and paramagnetic insulating (PMI) phases coexist and strongly compete with each other.[20,21] According to the phenomenological model

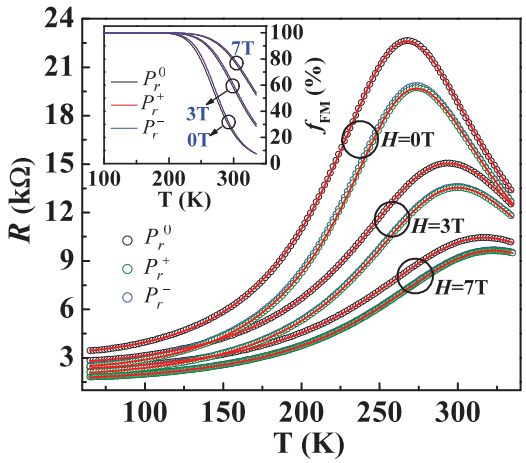


FIG. 3. Temperature dependence of resistance for the LBMO film under $H = 0$, 3 and 7 T, when PIN-PMN-PT is in the $P_r^0$, $P_r^+$, and $P_r^-$ states. Red solid lines are the fitted results using Eqs. (1) and (2). Inset: temperature dependence of $f_{FMM}$ under $H = 0$, 3 and 7 T, when PIN-PMN-PT is in the $P_r^0$, $P_r^+$, and $P_r^-$ states.

describing phase separation in perovskite manganites, the total resistance ($R$) of LBMO film can be considered as a serial combination of the resistances of coexisting phases[22]

$$R = f_{FMM}R_{FMM} + (1 - f_{FMM})R_{PMI}, \quad (1)$$

where $f_{FMM}$ and $(1 - f_{FMM})$ are the volume fractions, $R_{FMM}$ and $R_{PMI}$ are the resistances of the FMM and PMI phases, respectively. $R_{FMM}$ is related to the residual resistance $R_0$, single-magnon's scattering term $AT^2$ and electron-phonon interaction term $BT^5$ and can be expressed as $R_{FMM}(T) = R_0 + AT^2 + BT^5$, where $A$ and $B$ are constants.[23] For $T > T_C$, the temperature dependence of resistance can be described by $R_{PMI}(T) = C\exp[(T_0/T)^{1/4}]$, derived from the variable-range hopping model. Here, $T_0$ is a characteristic temperature and $C$ is a constant. The temperature dependence of $f_{FMM}$ obeys a two energy level Boltzmann distribution and can be written as[22]

$$f_{FMM} = \frac{1}{1 + \exp(\Delta U/k_B T)}, \quad (2)$$

where $\Delta U$ ($\Delta U = -U_0[1 - T/T_C^{\mathrm{mod}}]$) is the energy difference between the FMM and PMI phases, here $T_C^{\mathrm{mod}}$ (close to $T_C$) is the insulator-to-metal transition temperature used in the phenomenological model, and $U_0$ is the energy difference between the FMM and PMI phases at $T = 0$ K. The temperature dependence of resistance under different magnetic fields for the $P_r^0$, $P_r^+$, and $P_r^-$ states are fitted well across the entire temperature range using Eqs. (1) and (2), indicating that the electronic transport properties can be described by the phase separation model. Using the fitting parameters listed in Table I (see supplemental material[24]), the temperature dependence of $f_{FMM}$ can be calculated and is shown in the inset of Fig. 3. $f_{FMM}$ is significantly enhanced near $T_C$ by the magnetic field and poling-induced strain. Such enhancement has a dramatic impact on the strain-tunability of resistance, which is discussed later.

The strain-induced resistance change $(\Delta R)_{strain}$, $[(\Delta R)_{strain} = R(P_r^0, H) - R(P_r^+.H)]$, is shown in the inset (a) of Fig. 4. $(\Delta R)_{strain}$ exhibits a maximum value at around $T_C$, manifesting a strong correlation between the strain effect and the phase separation, i.e., the stronger the phase separation, the larger the strain-induced change in resistance.[25] To further understand the relationship between strain effect and phase separation, the temperature dependence of strain-induced relative change in resistance $(\Delta R/R)_{strain}$ (i.e., strain-tunability of resistance), here $(\Delta R/R)_{strain} = [R(P_r^0, H) - R(P_r^+, H)]/R(P_r^0, H)$, under $H = 0$, 1, 3, 5, and 7 T is shown in Fig. 4. $(\Delta R/R)_{strain}$ is significantly affected by the magnetic field and there is an intersection near $T_C$ between the $(\Delta R/R)_{strain}$ versus $T$ curve for $H = 0$ and that for $H = 1$, 3, 5, and 7 T. That is, the applied magnetic field enhances the strain effect above $T_C$, while weakens it below $T_C$. For example, at $T = 150$ K (much lower than $T_C$), $(\Delta R/R)_{strain}$ decreases from 26.1% to 20.2% when $H$ increases from 0 to 7 T. At $T = 300$ K (higher than $T_C$), $(\Delta R/R)_{strain}$ increases from 7.7% to 9.9% when $H$ increases from 0 to 7 T. Further details of the magnetic field dependence of $(\Delta R/R)_{strain}$ are shown in the inset (b) of Fig. 4. The isothermal $(\Delta R/R)_{strain}$ decreases with increasing $H$ for $T < T_C$ (e.g., $T = 65$, 135, and 200 K), and increases with increasing $H$ for $T > T_C$ (e.g., $T = 300$ and 330 K). At $T = 265$ K (around $T_C$), $(\Delta R/R)_{strain}$ is initially strengthened by the magnetic field but then weakened with further field increase. These findings are consistent with those shown in Fig. 4 and confirm the strong coupling between the magnetic field and the lattice strain in the LBMO film, which can be interpreted in terms of phase separation. Specifically, competition between the FMM and PMI phases is strongest at $T_C$.[20–22] The magnetic field modifies the subtle balance between these two phases by converting a considerable amount of $f_{PMI}$ to $f_{FMM}$. Here, the quantity $\lambda_T$ [$\lambda_T = f_{FMM}(T)/f_{PMI}(T)$] is defined to qualitatively characterize the magnitude of phase separation. Understandably, the closer $\lambda_T$ to $\lambda_{T_C}$, the stronger the phase separation, no matter whether $\lambda_T$ is larger or smaller than $\lambda_{T_C}$. The PMI phase dominates at high temperature, so $\lambda_T$ for $T > T_C$ is smaller than $\lambda_{T_C}$. When the LBMO film is subjected to a magnetic field, $\lambda_T$ becomes closer to $\lambda_{T_C}$ because of the increase in $f_{FMM}$ and

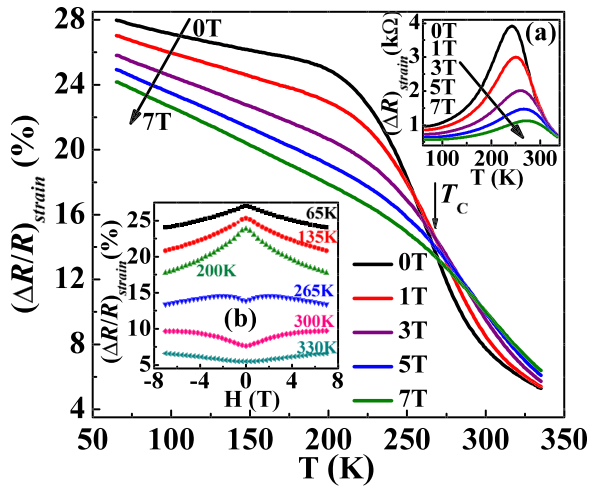


FIG. 4. $(\Delta R/R)_{strain}$ as a function of temperature under $H = 0$, 1, 3, 5, and 7 T. Inset (a) shows $(\Delta R)_{strain}$ as a function of temperature under $H = 0$, 1, 3, 5, and 7 T. Inset (b) shows $(\Delta R/R)_{strain}$ versus $H$ curves at temperatures as stated.

decrease in $f_{PMI}$. $(\Delta R/R)_{strain}$) for $T > T_C$ is thus enhanced because of the enhanced phase separation. On the contrary, at low temperatures, the FMM phase dominates over the PMI phase, $\lambda_T$ is larger than that of $\lambda_{T_C}$, and $\lambda_T$ may even exceed $\lambda_{T_C}$ under magnetic fields. Consequently, the magnetic field weakens phase separation and hence the strain effect.

The poling-induced remnant strain also significantly affects the magnetic properties of LBMO film. Fig. 5 shows the temperature dependence of the magnetization ($M$) of the LBMO film when the PIN-PMN-PT substrate is in different polarization states. The $M$ versus temperature ($T$) curves for the $P_r^0$ and $P_r^+$ (or $P_r^-$) states overlap at $T \sim 175$ K, suggesting opposite effects of the remnant strain on $M$ above and below 175 K. $T_C$ and $M$ for $T > 175$ K are both enhanced after poling, whereas $M$ is suppressed for $T < 175$ K, i.e., $M$ of the $P_r^+$ or $P_r^-$ states becomes smaller than that of the $P_r^0$ state for $T < 175$ K. To better understand this magnetic behavior, in-plane magnetic hysteresis loops are shown in Fig. 6. The remnant $M$ follows the trend of the $M$-$T$ curves in Fig. 5. At $T = 10$ K, a rectangular hysteresis loop is observed for the $P_r^0$ state. After PIN-PMN-PT has been poled to $P_r^+$ state, the remnant $M$ decreases, accompanied by a change in magnetic anisotropy, as illustrated by the change in the shape of the $M$-$H$ loop.[26] Furthermore, a modification of coercive field $H_C$ for the two polarized states is observed with diminishing divergence (see inset of Fig. 5) as temperature increases from 10 to 210 K. In our samples, electric field facilitates magnetization switching at low temperatures,[27] and enables significant coercive field modulation of up to 28.9% at $T = 10$ K. Associated with the polarization state switching from $P_r^+$ to $P_r^-$, $M$ almost remains unchanged. This provides further evidence that the polarization-switching-induced electrostatic doping has little effect on the magnetic properties. Therefore, the opposing effects of substrate poling on $M$ above and below the crossover temperature ($\sim$175 K) are concluded to be predominately strain-mediated, as in stark contrast to the charge-mediated opposite change in $M$ above and below the crossover temperature ($\sim$147 K) in $La_{1-x}Sr_xMnO_3$ ($x = 0.13$, 0.2)/$Pb(Zr_{0.2}Ti_{0.8})O_3$ heterostructures.[14,15,17]

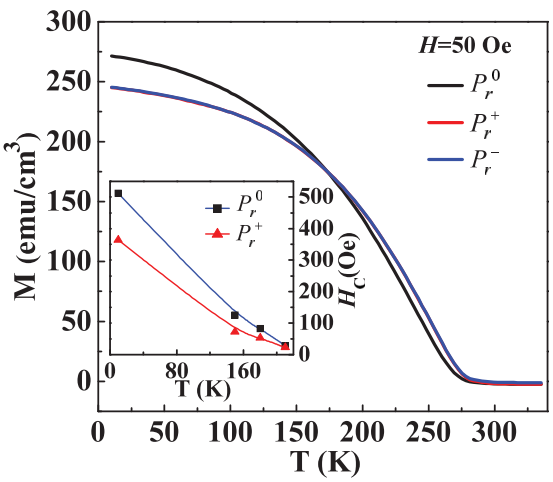


FIG. 5. Temperature dependence of field-cooled magnetization of the LBMO film under $H = 50$ Oe, when PIN-PMN-PT is in the $P_r^0$, $P_r^+$, and $P_r^-$ states. Inset shows the temperature dependence of the coercive field $H_C$ derived from Fig. 6.

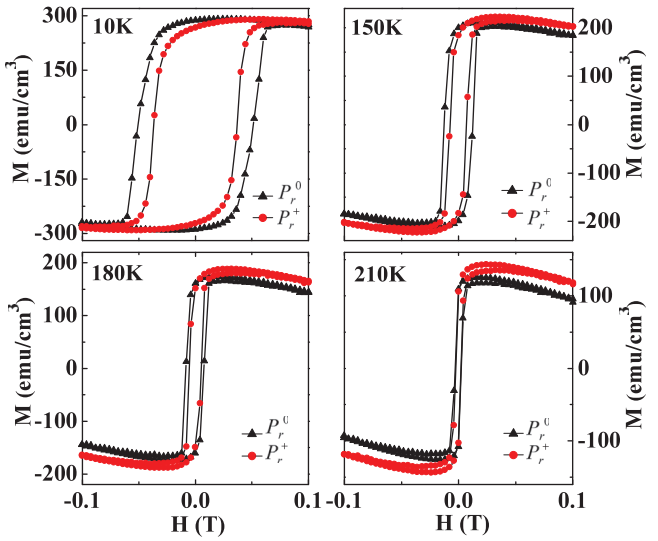


FIG. 6. In-plane magnetic hysteresis loops of LBMO/PIN-PMN-PT when PIN-PMN-PT is in the $P_r^0$ and $P_r^+$ states.

For a given temperature, the difference in magnetic properties between the $P_r^0$ and $P_r^+$ states verifies the magnetoelectric coupling in this system via magnetoelastic coupling at interface. Magnetoelastic energy generates uniaxial anisotropy,[26,28] and the stress anisotropy energy reads $E_{me} = K_{me}\cos^2\theta$, where $K_{me} = -\frac{3}{2}\lambda\sigma$, in which $\lambda$ is the magnetostriction coefficient converted from a negative to positive value with decreasing temperature for manganites,[29] $\sigma$ is the induced stress, and $\theta$ is the angle between $M$ and the $\sigma$-axis. Obviously, $K_{me} < 0$ favors $\theta = 0$, i.e., parallel alignment of $M$ relative to the stress axis, while $K_{me} > 0$ favors a perpendicular alignment with $\theta = \pi/2$. Based on this theory, the opposite effects of poling-induced strain on $M$ can be qualitatively explained. At relatively high temperatures, $\lambda$ is negative and $\sigma$ is positive under tensile stress. In this case, the substrate-induced in-plane tensile stress somewhat favors $M$ to be vertical to the film plane ($K_{me} > 0$). The poling of PIN-PMN-PT partly releases the tensile strain of the LBMO film and thus reduces the in-plane magnetoelastic anisotropy energy, leading to an increase in in-plane magnetization. At low temperatures, $\lambda$, the sign of which affects the magnetic easy axis orientation,[30] becomes positive. Thus, tensile strain favors an easy in-plane magnetization behavior ($K_{me} < 0$). Under this circumstance, the poling-induced reduction of tensile strain in LBMO film would cause less in-plane alignment of magnetization. Recent investigations on $Fe_3O_4$ films on ferroelectric $BaTiO_3$ substrates[31] and $Sr_2FeMoO_6$ films on various substrates with different static in-plane strain[32] suggest that the substrate-induced dynamic or static strain could alter the magnetic easy axis orientation and hence the magnetization of the $Fe_3O_4$ and $Sr_2FeMoO_6$ films via magnetoelastic coupling at interface.

In summary, LBMO films were epitaxially grown on (111)-oriented PIN-PMN-PT substrates. During ferroelectric poling along the [111] direction and polarization rotation, the variation in resistance of LBMO films tracks the electric-field-induced in-plane strain of substrates efficiently, demonstrating strain-mediated coupling. The magnetic field has opposing effects on the strain-tunability of resistance

$(\Delta R/R)_{strain}$ above and below $T_C$, which is explained on the basis of phase separation that is sensitive to poling-induced strain and magnetic field. Upon substrate poling, ferromagnetism of LBMO film is enhanced above the crossover temperature (~175 K) while suppressed below it, which is explained by magnetoelastic coupling at interface through modifying magnetic anisotropy. Our experiments indicate that the essential physics of phase separation in manganites can be further understood by measuring the strain-tunability of resistance under magnetic fields.

This work was supported by the National Basic Research Program of China (Grant Nos. 2012CB922003, 2009CB623304), NSFC (Grant Nos. 51172259, 50832007, 11090332), the CAS/SAFEA International Partnership Program for Creative Research Teams, and the PolyU internal grant (Grant No. G-U846).

[1]J. F. Wang, Y. C. Jiang, Z. P. Wu, and J. Gao, J. Appl. Phys. **113**, 17D911 (2013).
[2]C. Thiele, K. Dörr, O. Bilani, J. Roedel, and L. Schultz, Phys. Rev. B **75**, 054408 (2007).
[3]R. K. Zheng, H.-U. Habermeier, H. L. W. Chan, C. L. Choy, and H. S. Luo, Phys. Rev. B **80**, 104433 (2009).
[4]Y. J. Yang, Z. L. Luo, M. M. Yang, H. L. Huang, H. B. Wang, J. Bao, G. Q. Pan, C. Gao, Q. Hao, S. T. Wang, M. Jokubaitis, W. Z. Zhang, G. Xiao, Y. P. Yao, Y. K. Liu, and X. G. Li, Appl. Phys. Lett. **102**, 033501 (2013).
[5]Y. Yang, M. M. Yang, Z. L. Luo, H. Huang, H. Wang, J. Bao, C. Hu, G. Pan, Y. Yao, Y. Liu, X. G. Li, S. Zhang, Y. G. Zhao, and C. Gao, Appl. Phys. Lett. **100**, 043506 (2012).
[6]J. Wang, F. X. Hu, L. Chen, J. R. Sun, and B. G. Shen, J. Appl. Phys. **109**, 07D715 (2011).
[7]J. F. Wang, Y. C. Jiang, Z. P. Wu, and J. Gao, Appl. Phys. Lett. **102**, 071913 (2013).
[8]J. Wang, F. X. Hu, L. Chen, Y. Y. Zhao, H. X. Lu, J. R. Sun, and B. G. Shen, Appl. Phys. Lett. **102**, 022423 (2013).
[9]K. Dörr, O. Bilani-Zeneli, A. Herklotz, A. D. Rata, K. Boldyreva, J. W. Kim, M. C. Dekker, K. Nenkov, L. Schultz, and M. Reibold, Eur. Phys. J. B **71**, 361 (2009).
[10]Q. P. Chen, J. J. Yang, Y. G. Zhao, S. Zhang, J. W. Wang, M. H. Zhu, Y. Yu, X. Z. Zhang, Z. Wang, B. Yang, D. Xie, and T. L. Ren, Appl. Phys. Lett. **98**, 172507 (2011).
[11]W. Eerenstein, M. Wiora, J. L. Prieto, J. F. Scott, and N. D. Mathur, Nature Mater. **6**, 348 (2007).
[12]A. Alberca, C. Munuera, J. Tornos, F. J. Mompean, N. Biskup, A. Ruiz, N. M. Nemes, A. de Andres, C. Leon, J. Santamaria, and M. Garcia-Hernandez, Phys. Rev. B **86**, 144416 (2012).
[13]M. K. Lee, T. K. Nath, C. B. Eom, M. C. Smoak, and F. Tsui, Appl. Phys. Lett. **77**, 3547 (2000).
[14]C. A. F. Vaz, J. Hoffman, Y. Segal, J. W. Reiner, R. D. Grober, Z. Zhang, C. H. Ahn, and F. J. Walker, Phys. Rev. Lett. **104**, 127202 (2010).
[15]H. J. A. Molegraaf, J. Hoffman, C. A. F. Vaz, S. Gariglio, D. van der Marel, C. H. Ahn, and J.-M. Triscone, Adv. Mater. **21**, 3470 (2009).
[16]H. Lu, T. A. George, Y. Wang, I. Ketsman, J. D. Burton, C. W. Bark, S. Ryu, D. J. Kim, J. Wang, C. Binek, P. A. Dowben, A. Sokolov, C. B. Eom, E. Y. Tsymbal, and A. Gruverman, Appl. Phys. Lett. **100**, 232904 (2012).
[17]P. M. Leufke, R. Kruk, R. A. Brand, and H. Hahn, Phys. Rev. B **87**, 094416 (2013).
[18]Z. G. Sheng, J. Gao, and Y. P. Sun, Phys. Rev. B **79**, 174437 (2009).
[19]Y. Y. Zhang, X. B. Li, D. A. Liu, Q. H. Zhang, W. Wang, B. Ren, D. Lin, X. Y. Zhao, and H. S. Luo, J. Cryst. Growth **318**, 890 (2011).
[20]M. Fäth, S. Freisem, A. A. Menovsky, Y. Tomioka, J. Aarts, and J. A. Mydosh, Science **285**, 1540 (1999).
[21]L. W. Zhang, C. Israel, A. Biswas, R. L. Greene, and A. Lozanne, Science **298**, 805 (2002).
[22]S. L. Yuan, Z. Y. Li, W. Y. Zhao, G. Li, Y. Jiang, X. Y. Zeng, Y. P. Yang, G. Q. Zhang, F. Tu, C. Q. Tang, and S. Z. Jin, Phys. Rev. B **63**, 172415 (2001).
[23]M. Jaime, P. Lin, S. H. Chun, M. B. Salamon, P. Dorsey, and M. Rubinstein, Phys. Rev. B **60**, 1028 (1999).
[24]See supplementary material at http://dx.doi.org/10.1063/1.4822269 for Table I.
[25]R. K. Zheng, Y. Wang, H. U. Habermeier, H. L. W. Chan, X. M. Li, and H. S. Luo, J. Alloys Compd. **519**, 77 (2012).
[26]J. Y. Kim, L. Yao, and S. Van Dijken, J Phys.: Condens. Matter **25**, 082205 (2013).
[27]M. Liu, J. Lou, S. Li, and N. X. Sun, Adv. Funct. Mater. **21**, 2593 (2011).
[28]S. Sahoo, S. Polisetty, C.-G. Duan, S. S. Jaswal, E. Y. Tsymbal, and C. Binek, Phys. Rev. B **76**, 092108 (2007).
[29]L. I. Koroleva, R. V. Demin, A. V. Kozlov, D. M. Zashcherinskii, O. Y. Gorbenko, A. R. Kaul, O. V. Melnikov, and Y. M. Mukovskii, J. Magn. Magn. Mater. **316**, E644 (2007).
[30]J. W. Wang, Y. G. Zhao, C. Fan, X. F. Sun, S. Rizwan, S. Zhang, P. S. Li, Z. Lin, Y. J. Yang, W. S. Yan, Z. L. Luo, L. K. Zou, H. L. Liu, Q. P. Chen, X. Zhang, M. H. Zhu, H. Y. Zhang, J. W. Cai, X. F. Han, Z. H. Cheng, C. Gao, D. Xie, and T. L. Ren, Appl. Phys. Lett. **102**, 102906 (2013).
[31]H. F. Tian, T. L. Qu, L. B. Luo, J. J. Yang, S. M. Guo, H. Y. Zhang, Y. G. Zhao, and J. Q. Li, Appl. Phys. Lett. **92**, 063507 (2008).
[32]C. Du, R. Adur, H. Wang, A. J. Hauser, F. Yang, and P. C. Hammel, Phys. Rev. Lett. **110**, 147204 (2013).